Phys. Status Solidi B **246**, No. 3, 570–575 (2009) / **DOI** 10.1002/pssb.200880549

physica status solidi b
www.pss-b.com
basic solid state physics

Electronic and optical properties of III-nitrides under pressure

N. E. Christensen[*,1], I. Gorczyca[2], R. Laskowski[3], A. Svane[1], R. C. Albers[4], A. N. Chantis[4], T. Kotani[5], and M. van Schilfgaarde[5]

[1] Department of Physics and Astronomy, University of Aarhus, 8000 Aarhus C, Denmark
[2] Institute of High Pressure Physics "Unipress", Polish Academy of Sciences, Sokolowska 29/37, 01-142 Warsaw, Poland
[3] Institute of Materials Chemistry, Technical University of Vienna, Getreidemarkt 9/165TC, 1060 Vienna, Austria
[4] Theoretical Division, Los Alamos National Laboratory, Los Alamos, New Mexico 87545, USA
[5] School of Materials, Arizona State University, Tempe, Arizona 85287-6006, USA

Received 4 June 2008, revised 30 September 2008, accepted 30 September 2008
Published online 10 December 2008

PACS 62.50.–p, 71.15.Mb, 71.15.Qe, 71.35.Cc, 78.55.Cr

[*] Corresponding author: e-mail nec@phys.au.dk, Phone: +45 8942 3666, Fax: +45 8612 0740

Results of theoretical studies of electronic and optical properties of III–V nitride compound semiconductors under pressure are presented. As representatives InN and AlN have been chosen, and for InN the pressure effects on the fundamental gap as well as the role of conduction-band filling are examined. Both the fundamental gap and the electron effective mass increase with pressure, but due to the strong non-parabolicity of the conduction band, the pressure coefficient of the mass decreases with electron concentration. Particular attention is paid to the electronic states in the gap region. The "local-density gap error" is avoided by performing *Quasi Particle self-consistent GW* calculations, which produce slightly too large gaps. Including in addition the missing electron–hole excitonic states and the gap renormalization due to electron–phonon interaction a gap reduction is obtained. The e–h correlations are deduced from solutions of the Bethe-Salpeter equation. These are further used to study excitonic states in the gap of AlN under pressure, and for the rocksalt phase a pressure induced delocalized → localized transition is predicted.

1 Introduction Until recently it was believed that the fundamental band gap of InN was around 2 eV. However, several newer experiments now indicate that the room-temperature value is much lower, $E_G \approx 0.6–0.7$ eV [1, 2]. GaN has a 3.5 eV gap and that of AlN is 6.2 eV. Therefore, by varying the composition of quaternary (AlGaIn)N alloys it is possible to tune the gap over a wide range, and this makes these systems attractive for application in opto-electronic devices operating over a spectral range from the deep infrared to the far ultraviolet. Figure 1 illustrates this behaviour for $In_xGa_{1-x}N$ [2, 3].

For InN it is only recently that high-quality samples have been prepared, which made new comparison between experiment and theory possible. In that context it is also important that new *ab initio* quantum-theoretical methods have been implemented, which allow comparisons between calculated fundamental quantities, such as gaps, effective masses, optical spectra including excitons, and experimental data.

The *Local Density Approximation* (LDA) [4] to the density-functional theory (DFT) [4] has been successfully applied in self-consistent electronic structure calculations as basis for predictions of ground-state properties like crystal structure, pressure-induced transformations, phonon spectra, magnetism etc. The LDA usually leads to some overbinding, the predicted equilibrium volumes being 2–5% too small (neglecting the ionic zero-point motion). However, in materials where narrow bands, like those of "semi-core" states (Zn-3d, Ga-3d, In-4d, for example) contribute to the bonding, the LDA over-binding is increased. The LDA cannot describe the correlation of the electrons in the rather localized semi-core states well, and they are placed at too high energies. This implies that the hybridization to the other valence states is overestimated. For Zn

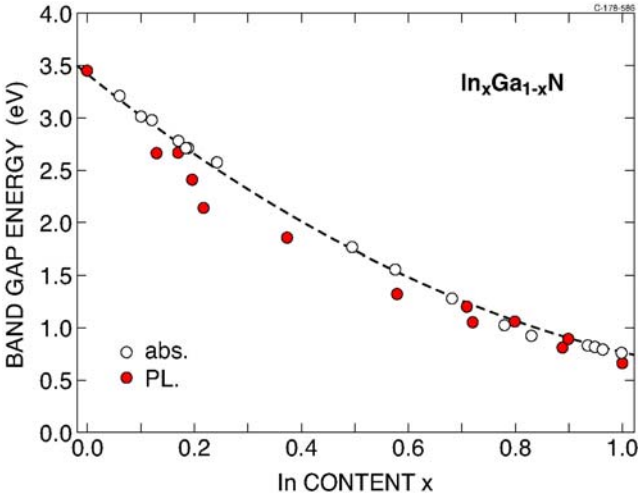

Figure 1 (online colour at: www.pss-b.com) InGaN alloy: Band gap vs. composition: absorption (abs) from [2], photoluminescence (PL) from [3].

LDA yields an equilibrium volume, which is 11% too small [6, 7]. Corrections for this can be made by down-shifting the semi-core states [6, 7] by LDA+U [8, 9] or applying self-interaction corrections (SIC) [10].

The DFT (LDA) is a total-energy method, and there is no reason to believe that the formal one-particle eigenvalues (band structures) are relevant for calculations of excitations, optical properties. In several cases the LDA spectra have turned out to be surprisingly similar to experimental results, but for semiconductors the well-known "LDA gap error" makes predictions from such calculations of excitation spectra very unreliable. A basic theory which may solve this problem was presented by Hedin [11] more than 40 years ago, the so-called GW method (G and W represent the Green's function and the screened Coulomb interaction, respectively). Hybertsen and Louie [12] implemented the GW approximation as a perturbation to the DFT using the LDA eigenfunctions (GW-LDA). This method was a major improvement, but it has been shown [13] that in several cases the LDA starting point for such calculations is poor, and that such a "one-shot" GW calculation often underestimates the band gaps and can fail seriously. This influence of the LDA calculation is eliminated in the *Quasiparticle self-consistent GW* (QSGW) method introduced by Kotani, van Schilfgaarde and Faleev, see [14] and references therein. The method is a many-body perturbation theory considered as an expansion around some non-interacting Hamiltonian H_0. A self-consistency procedure is used to construct an H_0, which is as close as possible to the interacting Hamiltonian.

Application of the (QSGW) to a large number of semiconductors has shown [15] that this method systematically gives semiconductor band gaps, which are larger than those measured in optical experiments. The reason for this is that several terms are not included in the expansion. For example are electron–hole (e–h) correlations, which contribute essentially to optical spectra, omitted. They reduce the gap and give rise to exciton states in the gap. Here we report calculations of excitonic effects obained by solution of the Bethe-Salpeter equation (BSE) [16, 17]. This is an extension of previous work on ZnO [9] and nitride semiconductors [18–21].

In the following we shall discuss results obtained for the two semiconductors InN and AlN. First, Section 2.1 summarizes the results obtained for n-doped InN with emphasis on the properties of the lowest conduction band (CB). Then, in Section 2.2, the band gaps, LDA vs. GW, are discussed, mainly for InN and AlN. The calculations of excitons in AlN under pressure follow in Section 2.3.

2 InN and AlN: calculated electronic and related properties

2.1 Conduction band and effective electron masses in InN Indium nitride crystallizes in the wurtzite structure at ambient conditions, and the structural parameters, u and c/a can be calculated with good precision by means of standard full-potential methods like linear muffin tin orbitals (FP-LMTO) [22] within the LDA. Also the pressure-induced wurtzite → rocksalt structural transformation at 10–12 GPa is found in agreement with experiments (for details, please see [23]).

The calculated band structure is shown in Fig. 2.

The minimum gap is direct, at the zone center, but a straight LDA calculation yields a *negative* gap, the Γ_1 state being below Γ_6. The present LDA+C approach includes correcting *ad hoc* potentials of the form in [24].

The adjusting potentials are added to each muffin-tin sphere. They are sharply peaked at the nuclear sites and act therefore mainly on the s-like states. In "empty spheres"

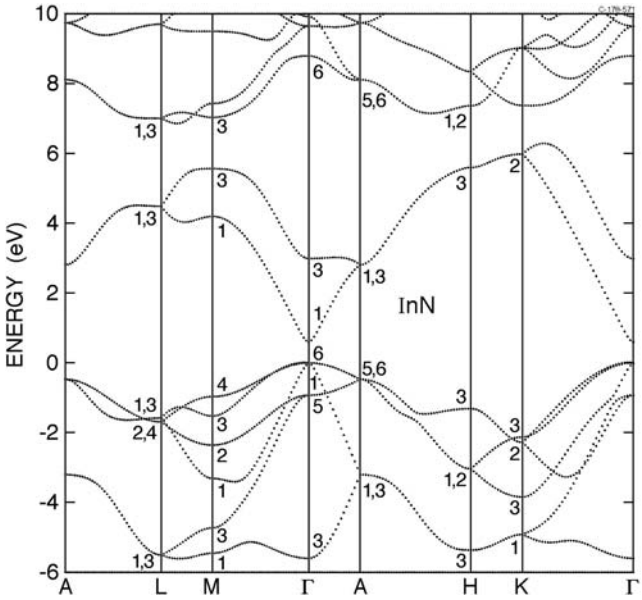

Figure 2 Calculated band structure of InN ("LDA + C"). The energy is zero at the valence band maximum. Scalar relativistic calculation (spin–orbit coupling omitted).

(interstitial positions in open structures) they are weak, but long range adjusting potentials are chosen, often just constant potentials. The parameters are chosen so that experimental gaps at symmetry points of the Brillouin zone are well reproduced. The success of such a procedure depends, of course, sensitively on the assignment of the optical data to transitions in the band structure. Due to the transferability of the potentials from atoms in simple structures to self-consistent calculations for supercells [23] and superlattices [25] this LDA+C method has been useful for calculations for complex, semi-conducting systems. The value of E_G in the band structure shown in Fig. 2 is 0.60 eV, and its pressure coefficient is 30 meV/GPa. This agrees well with experiments, 30 ± 1 meV/GPa [26] and 27.5 ± 1 meV/GPa [3, 27].

One of the consequences of the narrow gap of InN is the peculiar shape of the lowest CB, which even for rather small wavenumbers k deviates markedly from a parabolic dispersion relation. In n-type materials, where the donor levels are well above the conduction-band minimum, (CBM), the extra electrons form a degenerate Fermi gas with a Fermi level, E_F, above the CBM, and the absorption edge, E_{abs}, becomes larger than the fundamental gap (Burstein–Moss shift [28, 29]).

Figure 3 shows the energy, E_c, in the lowest CB as a function of the electron concentration, n_e, where E_F was derived by integration of the density-of-states function for the CB. Experimental values [30, 31] of E_{abs} are included in the figure. A comparison of E_{abs} and E_c is relevant because the large heavy-hole mass of InN and the steep increase of the CB with k, implies that dispersion of the upper valence band can be neglected in the analysis. The dotted curve in Fig. 3 shows that a parabolic model of the CB (fixed mass $m^* = 0.07m_0$, where m_0 is the free-electron mass) is an extremely poor approximation in this case. The dashed curve in Fig. 3, which was calculated for elevated pressure,

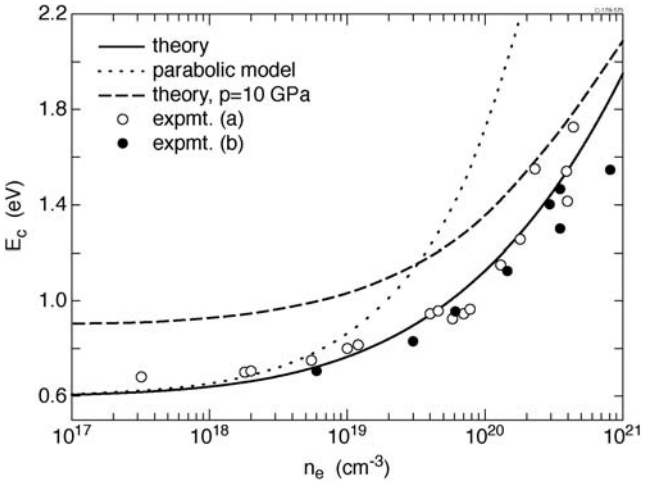

Figure 3 Calculated conduction-band energy versus free-carrier concentration (n_e). The experimental points represent the absorption edges, E_{abs}, as measured, [30] (a) and [31] (b). The dashed curve was calculated for a compressed crystal (p = 10 GPa).

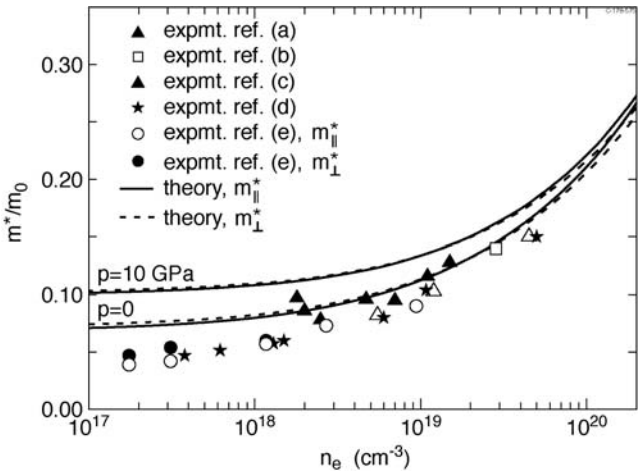

Figure 4 Calculated (curves) optical electron mass vs. electron concentration for $p = 0$ and 10 GPa. The points are from experiments, (a) [32], (b) [33], (c) [34], (d) [35], and (e) [36].

10 GPa (close to the transition to the rocksalt structure), shows that the absorption edge increases with pressure, but also that its pressure coefficient *decreases* as n_e is increased. This agrees with experimental results in Refs. [3] and [27], and it also reflects that the effective mass increases with pressure.

One effect of the non-parabolicity is that the *optical* and *curvature* effective masses are different, and for comparison to experiments it is therefore essential to choose the one which is relevant to the measurement [23]. The two masses have the same value at the CBM, but they differ as k is moved away from the zone center. The in-plane mass (Γ–M and Γ–K directions) is denoted by $m_\perp^*$, and the one corresponding to the c-axis by $m_\parallel^*$ (Γ–A). As can be seen from Fig. 4 $m_\perp^*$ and $m_\parallel^*$ are quite similar for InN.

The reported experimental masses (averaged) at $k = 0$ range from [34] $0.044m_0$ to [36] $0.085m_0$. The most reliable values are maybe 0.05 and $0.07m_0$ from Refs. [35] and [32], respectively. The present calculated average mass is $0.069m_0$, in the range of experimental results. Our calculations in [37] gave the value $0.075m_0$. The calculations in [37] were based on the LMTO-ASA (Atomic Spheres Approximation) [22]. This uses spherically symmetrical potentials inside atomic spheres, wheras this is not the case for the FP-LMTO used here.

For a discussion of the curvature mass, the reader is referred to [23], where it is shown that it increases rapidly with n_e, as also can be expected from the shape of the CB in Fig. 2. At some point it diverges and becomes negative, again a signature of the strong non-parabolicity of the CB in InN.

2.2 InN and AlN: beyond LDA The application of the adjusting potentials in the LDA + C method is useful, but it is an *ad hoc* method without a firm theoretical basis. The GW approximations [12, 13] represent significant improvements, and in Fig. 5 the LDA and QSGW bands for InN are compared. Only a small part of the CBs is included.

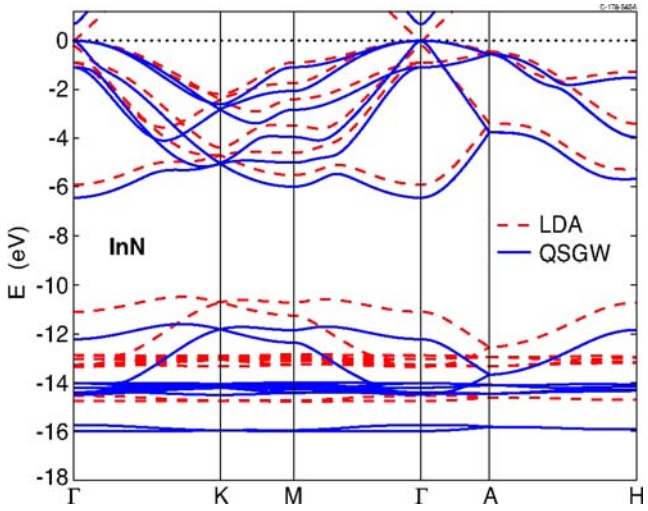

Figure 5 (online colour at: www.pss-b.com) LDA (dashed, red) and QSGW (full line, blue) bands of InN. Zero energy is at the valence band maximum.

The LDA gap is negative, but the GW bands of InN exhibit a positive gap, 1.04 eV. This is larger than the 0.7 eV gap found in optical experiments, and reasons for this over-estimate are given below. Figure 5 further shows that the rather narrow In-4d states have been pulled downwards in energy by the QSGW, i.e. another improvement over LDA.

Figure 6 shows a similar comparison for AlN. The LDA gap is 4.05 eV and with QSGW the calculated gap is 6.76 eV, i.e. ~0.5 eV larger than found in optical absorption measurements, or 0.64 eV larger than the 6.12 eV derived from time-resolved photoluminescence [38]. The spectra calculated with e–h correlations (BSE), see the dielectric functions obtained in [19], show that the e–h correlations enhance the intensities in the low-frequency regime. Further, these include the exciton states (almost smeared out in [19] due to broadening). In AlN the exciton binding energies are close to 0.1 eV. In addition electron–

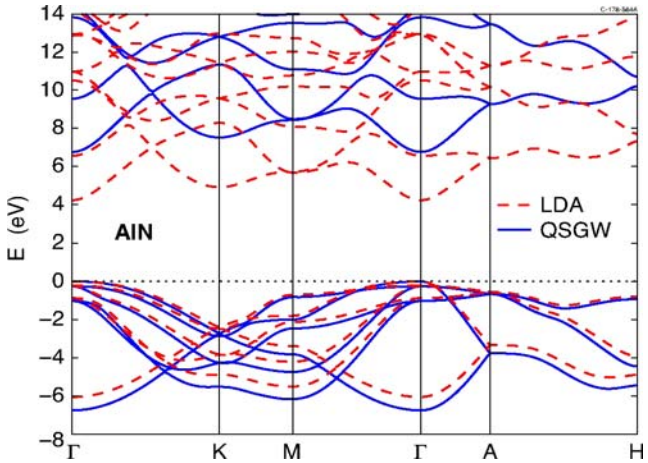

Figure 6 (online colour at: www.pss-b.com) AlN: LDA (dashed, red) and QSGW bands for AlN.

phonon interaction leads to a gap renormalization [39]. This can be significant, $\Delta E_0 = -239$ meV (Table III in [39]) in AlN, from zero-point motion alone (in diamond the gap is even reduced by 370 meV, [40]). For InN ΔE_0 ($T = 0$) is −178 meV or −68 meV, depending on the method used to determine the value [39]. The present calculations for AlN and InN did not include spin–orbit (SO) coupling. SO splitting at the VBM reduces the gaps further by a few meV. Finally, higher-order terms in the GW expansion may be significant. But the present, and other, results suggest that a BSE calculation based on QPGW should yield optical spectra for semiconductors in good agreement with experiments.

Exciton binding energies, i.e. the difference between the direct energy gap and the excitation energy, as calculated by the BSE formalism are not sensitive to the value of the gap in the 'input' quasiparticle band structure, since the gap is essentially cancelled by the diagonal term in the Hamiltonian, $\varepsilon_{c\boldsymbol{k}} - \varepsilon_{v\boldsymbol{k}} + \Delta$ in [20] (misprint in Eq. (3) in [20] and in (5) of [19]). For wurtzite AlN it was found [19] that Elliott's model fits the BSE results surprisingly well concerning the excitonic energies, $1/n^2$ scaling of the binding energies as in a hydrogen-like atomic model. Under hydrostatic pressure AlN transforms to the rocksalt structure (transition around $P_t = 13$ GPa). At this pressure the volume in the rocksalt phase is $V_{B1} \sim 80\%$ of the zero-pressure volume of wurtzite AlN. At this volume the three lowest states in the gap have the binding energies 0.115 eV, 0.049 eV, and 0.013 eV, i.e. no $1/n^2$ scaling, and thus quite different from wurtzite AlN. Compressing B_1-AlN further the binding energies were found to vary as shown in Table 1. For low compressions there is a slight increase in binding energy due to decreasing screening (increasing direct gap). Between 5% and 10% compression there is a jump in the energies, and for higher compression they *decrease*.

The jump in binding energies is associated with a change of the localization of the exciton wavefunction. From the BSE eigenvectors a weight distribution in k-space can be calculated [21], and Fig. 7 shows this function for $\Delta V = -5\%$ and -10%. At high compressions the excitons are spread over a large volume in k-space; from a rather localized state a transition to a delocalized state has occurred. The situation in configuration space is opposite: a pressure induced transition from delocalized to more localized excitons occurs. This is illustrated in Fig. 8 where the real-space distribution is shown (for a definition of Φ, please see [21]). The transition is related to a pressure-induced change in topology of the one-particle band struc-

Table 1 Binding energies in eV for the three lowest excitons in B_1-AlN for different volumes.

$\Delta V/V_{B1}$	0	−5%	−10%	−15%
1	0.115	0.126	0.218	0.207
2	0.049	0.052	0.111	0.106
3	0.013	0.017	0.066	0.059

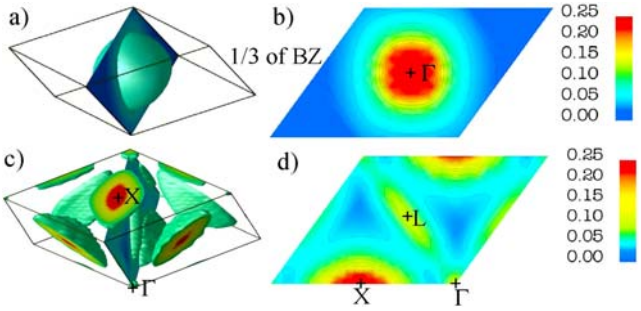

Figure 7 (online colour at: www.pss-b.com) *k*-space weight distribution calculated for the lowest excitonic states for $\Delta V = -5\%$ ((a) and (b)) and $\Delta V = -10\%$ ((c) and (d)) 1/3 of the BZ is shown.

tures. At low pressure the direct gap is at Γ, whereas the X-gap becomes the lowest direct gap at high pressure. The Γ-gap increases with pressure [21], and the increase in binding energy going from 0% to 5% compression (Table 1) agrees qualitatively with what is expected for Wannier excitons due to the decrease in screening. A similar argument does not apply to the more localized excitons, compressions 10% and 15% (Table 1). Although the excitons at low pressure in B_1-AlN are rather delocalized, they are still not as delocalized as at zero pressure in the wurtzite phase. Thus, in B_1-AlN, even at low pressure, they are not "good" Wannier excitons, and they do not follow Elliott's $1/n^2$-rule.

At high pressure, the B_1-AlN excitons are rather localized in real space, but not "really good" Frenkel excitons.

Figures 8a and b include four curves. Two of these have large $|\Phi|$ values. These correspond to the cases where (blue, dashed): the hole is on N, electron on N and (red, dotted): hole on N and e on Al. Since the amplitudes of the green and black curves are vanishingly small, it follows that the hole is always on nitrogen atoms, whereas the electron can be on both kinds of atoms. This is not surprising: Hole states originate in states at the valence-band top, predominantly of N (p) type, whereas the conduction electron states have large N as well as Al (s) components.

3 Concluding remarks Theoretical predictions of optical excitations in solids require that electron–electron and electron–hole correlations are taken into account. Separate QSGW and BSE calculations were presented. It should be interesting, in the future, to combine the two approaches in one implementation. However, in their present implementations, both schemes require substantial computing resources. This also means that neither of the methods is practical for calculations for large supercells and superlattices. For such cases we still use *ad-hoc* methods like LDA+C to obtain reasonable band gap values.

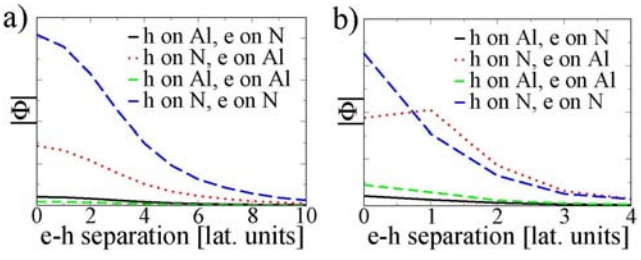

Figure 8 (online colour at: www.pss-b.com) Real-space distribution of the lowest excitons, (a) $\Delta V = -5\%$ and (b) $\Delta V = -10\%$. Note the difference in length scales in (a) and (b).

Acknowledgement MvS and TK acknowledge support by ONR contract N00014-07-1-0479.

References

[1] V. Yu. Davydov, A. A. Klochikhin, R. P. Seisan, V. V. Emtsev, S. V. Ivanov, F. Bechstedt, J. Furthmüller, H. Harima, A. V. Mudrui, J. Aderhold, O. Semchinova, and J. Graul, Phys. Status Solidi B **229**, R1 (2002).
[2] J. Wu, W. Walukiewicz, K. M. Yu, J. W. Ager III, E. E. Haller, H. Lu, W. Schaff, Y. Saito, and Y. Nanishi, Appl. Phys. Lett. **80**, 3967 (2002).
[3] G. Franssen, I. Gorczyca, T. Suski, A. Kaminska, J. Pereiro, E. Muñoz, E. Ilipoulos, A. Georgakilas, S. B. Che, Y. Yoshikawa, N. E. Christensen, and A. Svane, J. Appl. Phys. **103**, 033514 (2008).
[4] W. Kohn and L. J. Sham, Phys. Rev. **140**, A1133 (1965).
[5] P. Hohenberg and W. Kohn, Phys. Rev. **136**, B864 (1964).
[6] N. E. Christensen and D. L. Novikov, Int. J. Quantum Chem. **77**, 880 (2000).
[7] N. E. Christensen, in: High Pressure in Semiconductor Physics I, T. Suski and W. Paul (eds.), Vol. 54, Semiconductors and Semimetals, edited by R. K. Willardson and E. R. Weber (Academic Press, 1998), p. 49.
[8] A. I. Liechtenstein, V. I. Anisimov, and J. Zaanen, Phys. Rev. B **52**, R5467 (1995).
[9] R. Laskowski and N. E. Christensen, Phys. Rev. B **73**, 45201 (2006).
[10] A. Svane, Phys. Rev. B **53**, 4275 (1996).
[11] L. Hedin, Phys. Rev. **139**, A796 (1965).
[12] M. S. Hybertsen and S. G. Louie, Phys. Rev. B **34**, 5390 (1986).
[13] M. van Schilfgaarde, T. Kotani, and S. V. Faleev, Phys. Rev. B **74**, 245125 (2006).
[14] T. Kotani, M. van Schilfgaarde, and S. V. Faleev, Phys. Rev. B **76**, 165106 (2007).
[15] M. van Schilfgaarde, T. Kotani, and S. V. Faleev, Phys. Rev. Lett. **96**, 226402 (2006).
[16] L. J. Sham and T. M. Rice, Phys. Rev. **144**, 708 (1966).
[17] S. Albrecht, G. Onida, and L. Reining, Phys. Rev. B **55**, 10278 (1977).
[18] R. Laskowski and N. E. Christensen, Phys. Rev. B **72**, 035204 (2005).
[19] R. Laskowski and N. E. Christensen, Phys. Rev. B **74**, 075203 (2006).
[20] R. Laskowski and N. E. Christensen, Phys. Status Solidi B **244**, 17 (2007).
[21] R. Laskowski and N. E. Christensen, Phys. Rev. B **75**, 201202 (2007) (RC).
[22] O. K. Andersen, Phys. Rev. B **12**, 3060 (1975).
[23] I. Gorczyca, J. Plesiewicz, L. Dmowski, T. Suski, N. E. Christensen, A. Svane, C. S. Gallinat, G. Koblmueller, and J. S. Speck, J. Appl. Phys. **104**, 013704 (2008).

[24] N. E. Christensen, Phys. Rev. B **30**, 5753 (1984).
[25] M. Cardona, T. Suemoto, N. E. Christensen, T. Isu, and K. Ploog, Phys. Rev. B **36**, 5906 (1987).
[26] S. X. Li, J. Wu, E. E. Haller, W. Walukiewicz, W. Shan, H. Lu, and W. J. Schaff, Appl. Phys. Lett. **83**, 4963 (2003).
[27] A. Kaminska, G. Franssen, T. Suski, I. Gorczyca, N. E. Christensen, A. Svane, A. Suchocki, H. Lu, W. J. Schaff, E. Dimakis, and A. Georgakilas, Phys. Rev. B **76**, 075203 (2007).
[28] E. Burstein, Phys. Rev. **93**, 632 (1954).
[29] T. S. Moss, Proc. Phys. Soc. (London) B **67**, 775 (1964).
[30] J. Wu and W. Walukiewicz, Superlattices Microstruct. **34**, 63 (2003).
[31] A. G. Bhuiyan, K. Sugita, K. Kasahima, A. Hashimoto, A. Yamamoto, and V. Yu. Davydov, Appl. Phys. Lett. **83**, 4788 (2003).
[32] J. Wu, W. Walukiewicz, W. Shan, K. M. Yu, J. W. Ager, E. E. Haller, H. Lu, and W. J. Schaff, Phys. Rev. B **66**, 201403 (2002).
[33] A. Kasic, M. Schubert, Y. Nanishi, and G. Wagner, Phys. Rev. B **65**, 115206 (2002).
[34] T. Inushima, M. Higashiwaki, and T. Matsui, Phys. Rev. B **68**, 235204 (2003).
[35] S. P. Fu and Y. F. Chen, Appl. Phys. Lett. **85**, 1523 (2003).
[36] T. Hofmann, T. Chavdarov, V. Darakchieva, H. Lu, W. J. Schaff, and M. Schubert, Phys. Status Solidi C **3**, 1854 (2006).
[37] I. Gorczyca, L. Dmowski, J. Plesiewicz, T. Suski, N. E. Christensen, A. Svane, C. S. Gallinat, G. Koblmueller, and J. S. Speck, Phys. Status Solidi B **245**, 887 (2008).
[38] J. Li, K. B. Nam, M. L. Nakarmi, J. Y. Lin, H. X. Jiang, P. Carrier, and S.-H. Wei, Appl. Phys. Lett. **83**, 5163 (2003).
[39] M. Cardona and M. L. W. Thewalt, Rev. Mod. Phys. **77**, 1173 (2005).
[40] M. Cardona, T. A. Meyer, and M. L. W. Thewalt, Phys. Rev. Lett. **92**, 196403 (2004).